Stanford Exploration Project, Report 129, May 6, 2007, pages 95–109

Seismic monitoring of sub-salt reservoirs: Time-lapse wave-equation inversion

Gboyega Ayeni and Biondo Biondi

ABSTRACT

Time-lapse seismic is now a core technology for reservoir monitoring and characterization. However, many challenges continue to exist in its application in complex geology (e.g. sub-salt reservoirs). Differences in acquisition geometry (non-repeatability) and poor illumination are examples of factors that cause contamination of the desired time-lapse effects (i.e. changes due to production). By computing the time-lapse response as a difference between least-squares inverse images or posing time-lapse imaging as a least-squares inverse problem, we hope to attenuate geometry and other unwanted effects.

INTRODUCTION

Time-lapse (or 4D) seismic monitoring of hydrocarbon reservoirs has seen tremendous growth throughout the 1990s and during this decade. In general, 4D seismic is based on the premise that changes in fluid content (e.g. due to production) cause changes in the acoustic properties of rocks which are detectable in recorded seismic data. A detailed review of the seismic properties of reservoir pore-fluids is given by Batzle and Wang (1992). Lumley (1995) gives a comprehensive review of the theory, caveats and applications of time-lapse seismic in reservoir monitoring. Also, in his review of methods and current applications of 4D seismic, Calvert (2005) outlined many of the acquisition, processing modeling and integration requirements for successful application of the technology. Since its adoption as a monitoring tool, many successful applications of time-lapse seismic monitoring have been published (Biondi et al., 1998; Lefeuvre et al., 2003; Whitcombe et al., 2004; Zou et al., 2006).

Repeatability is a major consideration for successful application of 4D seismic monitoring, especially in reservoirs with very low seismic responses. Non-repeatability may result from differences in survey acquisition geometry and binning, cable feathering, tides, source-wavelet bandwidth and phase variability, differential static time-shifts, ambient noise, residual multiple energy, and relative mispositioning of imaged reflection events (Rickett and Lumley, 2001; Johnston, 2005). Laws and Kragh (2000) and Eiken et al. (2003) discuss acquisition techniques that may reduce some of these uncertainties. Recent advances in time-lapse processing have improved the success rate in 4D seismic monitoring. Some of the common processing issues are discussed by Ross and Altan (1997) and Eastwood et al. (1994). Rickett and Lumley (2001) outline a cross-equalization scheme involving spatial re-alignment, matched filtering,

amplitude balancing and warping. Co-processing or parallel processing (involving controlled amplitude and phase, early geometry equalization, and application of the same algorithms and parameters) of the different seismic datasets is now common practice (Johnston, 2005).

Although some of the best practices in time-lapse reservoir monitoring help improve the the reliability of time-lapse responses and confidence in their interpretations, many loopholes still exist. Most of these shortcomings may not be important in reservoirs with large seismic responses — where such unwanted effects are submerged by the much stronger time-lapse response. However, in many scenarios (e.g. sub-salt reservoirs), slight inaccuracies may cause considerable spurious 4D effects. We envisage that with the gradual increase in demand for more optimal reservoir management (hence the need for more accurate amplitudes), and current changes in acquisition patterns (hence the need to utilize surveys with potentially widely varying geometries), circumventing the shortcomings in current time-lapse imaging practice will be necessary.

We briefly discuss some of the challenges in sub-salt reservoir monitoring and show preliminary (raw) 2D synthetic time-lapse images in the presence and absence of salt. Our goal is to attenuate contamination by artifacts caused by differences in acquisition geometries and also to correct for the weakened time-lapse response due to limited illumination. We discuss two target-oriented least-squares inversion approaches that may overcome some of these challenges.

In the first approach, based on previous work by Valenciano et al. (2006), the time-lapse image is given as the difference between two least-squares inverse images. In the second approach, we pose time-lapse imaging as an inverse problem and propose to directly solve for the time-lapse image by least-squares inversion. By solving for the time-lapse image through inversion rather than as a difference between migrated seismic surveys, we believe many undesired effects in seismic monitoring of sub-salt reservoirs — and reservoirs with very complex overburdens — could be removed.

SUBSALT RESERVOIR MONITORING

The large velocity contrast at salt boundaries, complexity of seismic travel paths, lack of amplitude reciprocity, and effects from peaks and pits (Muerdter and Ratcliff, 2001) are some of the causes of illumination problems in sub-salt reservoirs. Several acquisition techniques (wide-, rich-, and full-azimuth surveys, ocean-bottom surveys and VSPs) now help improve illumination of subsalt reservoirs (Sava, 2006). Also, 3D prestack depth migration (PSDM) has been shown to be an important processing tool for sub-salt imaging (Ratcliff et al., 1994; Biondi et al., 1999; Malaguti et al., 2001).

Although many advanced acquisition and processing techniques help to correctly image reflectors beneath most complex/detached and/or steeply dipping salt bodies, the seismic amplitudes recovered from most of these techniques are not usually reliable. Rickett (2003) suggested weighting functions derived from reference images to correct for amplitude distortions caused by illumination problems. While amplitudes recovered from such normalization

schemes meet many imaging requirements, their reliability may be considerably lower in scenarios such as sub-salt reservoir monitoring where slight inaccuracies could be very important. As shown in Figure 1, slight changes in shot/image position (and/or acquisition geometry) could result in widely different (and complex) travel paths of sub-salt reflections. Also, artifacts from the migration process tend to obscure the weak signals from these reflectors (Clapp, 2005) and even small differences between these artifacts may considerably contaminate the time-lapse response. In many cases, there is no guarantee that the cross-equalization process would leave the desired time-lapse effect intact. These factors, coupled with the original illumination problem, make subsalt reservoir monitoring a difficult task.

2D NUMERICAL EXAMPLE

2D synthetic data were generated for the two sets of simple velocity models (Figure 2) using by acoustic finite difference modeling. Changes in fluid content due to production are modeled as an increasing Gaussian velocity anomaly located at (x = 0 m, z = 600 m). In each case, we modeled end-on surveys consisting of 201 shots (range: -2000 m to 2000 m, shot spacing: 20 m, receiver spacing: 20 m, maximum offset: 1200 m) in opposite directions.

The datasets were migrated using a shot-profile migration algorithm (an adjoint to the forward-modeling operation). By using exactly the same processing parameters, we preclude frequency, bandwidth and phase differences. Migrated images — using the correct model velocities — are shown in Figures 3 and 4. Since the actual velocity models are not usually known, it is common practice to migrate the datasets with the same velocity (e.g. baseline) model. Raw difference images obtained using different velocity fields are shown in Figures 5 and 6. For exactly the same acquisition geometry, the time-lapse response in the presence of the salt wedge (Figure 5b) is relatively weaker and much more complicated than when no salt is present (Figure 5a). Also, as seen in Figures 5c and d, a change in the acquisition geometry introduces more artifacts into time-lapse image when the salt wedge is present. These effects result partly from the poor illumination close to the salt flank, unequal illumination of the salt flank (due to the difference in survey direction) and contamination by differences in the relatively much stronger migration artifacts. As shown in Figure 6, using an incorrect velocity field introduces a different pattern of artifacts when the salt wedge is present. Thus, since exact velocities are not used in practice, any assumptions made with regards to the migration velocities may be difficult to account for. In the absence of the salt wedge, the results are much less complicated and simple cross-equalization of the surveys should suffice. While opposite acquisition directions may be an extreme, surveys over very complex salt bodies acquired with slightly different geometries may result in highly deteriorated time-lapse images even after careful cross-equalization.

TIME-LAPSE IMAGING AS AN INVERSE PROBLEM

(Tarantola, 1987; Claerbout, 2004) discuss the use of geophysical inversion as an imaging tool. In recent applications, inverted seismic images are computed by weighting the migra-

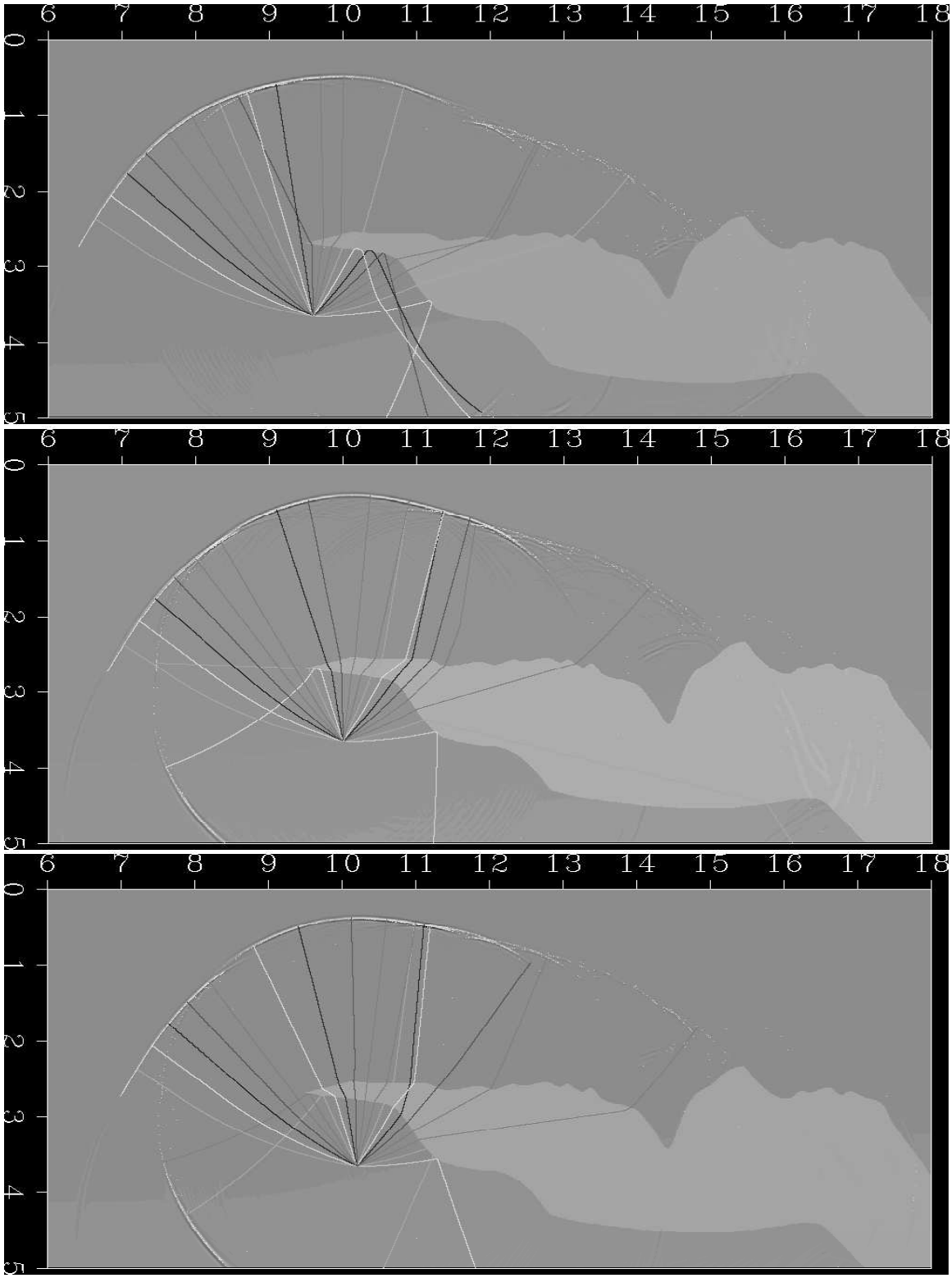

Figure 1: Subsalt Illumination effects: wave-field/ray-tracing modeling. Notice the dramatic changes in raypaths as the image point shifts from left (top) to right (bottom). gayeni1-Biond_Ray [NR]

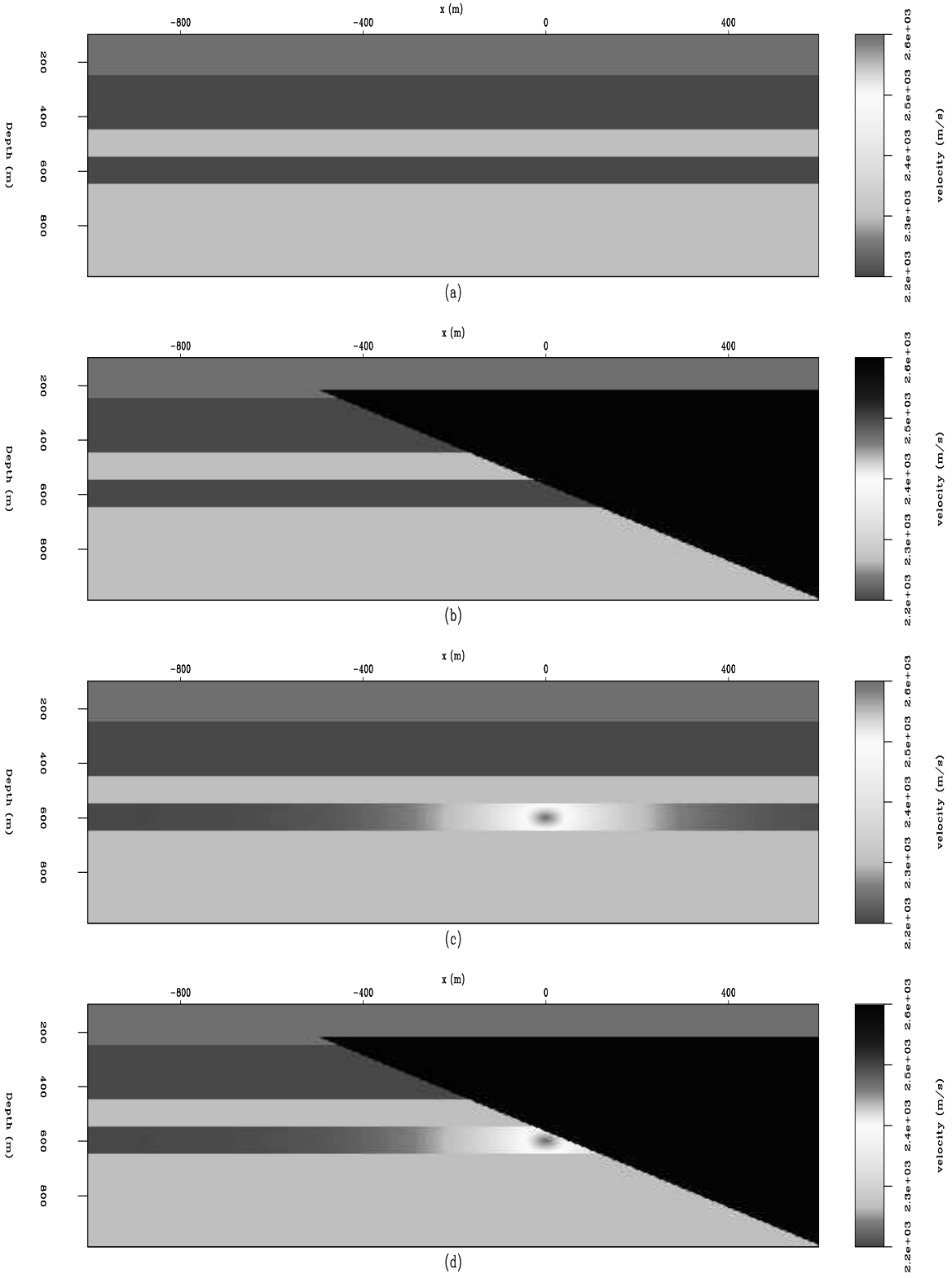

Figure 2: Velocity models for (a) and (b) Baseline, (c) and (d) Monitor surveys. Velocity from top: 2500, 2350, 2300, 2350, 2300m/s; salt velocity: 4500 m/s. Velocity change between surveys: +200m/s. gayeni1-Gboye_2DVel [ER]

tion result with the inverse of the Hessian matrix. The associated large computational cost and complexity makes the explicit computation of the Hessian matrix and its inverse impracticable. Valenciano et al. (2006) demonstrate that by taking the sparsity of the Hessian into account, the inverse of the Hessian matrix may be computed cheaply and applied in a target-oriented manner. This approach appears to yield better results than simple migration in subsalt reservoirs. For the time-lapse problem, one approach would be to to compute the time-lapse image as a difference between inverse images computed as described above. Another approach would be to solve for the time-lapse image through inversion rather a difference between images.

Given a linear modeling operator $\mathbf{L}$, the synthetic data $\mathbf{d}$ is computed using $\mathbf{d} = \mathbf{L}\mathbf{m}$, where $\mathbf{m}$ is a reflectivity model. Two different surveys (say a baseline and monitor) may be represented as follows:

$$\mathbf{L}\mathbf{m}_0 = \mathbf{d}_0,$$

$$\mathbf{L}\mathbf{m}_1 = \mathbf{d}_1, \tag{1}$$

where $\mathbf{m}_0$ and $\mathbf{m}_1$ are the reflectivity models at the time we acquire the datasets, ($\mathbf{d}_0$ and $\mathbf{d}_1$) respectively. Taking $\mathbf{L}_0$ and $\mathbf{L}_1$ to be the modeling operators for two different surveys, the quadratic cost functions are defined as

$$S(\mathbf{m}) = \|\mathbf{L}_0\mathbf{m}_0 - \mathbf{d}_0\|^2,$$

$$S(\mathbf{m}) = \|\mathbf{L}_1\mathbf{m}_1 - \mathbf{d}_1\|^2. \tag{2}$$

The least-squares solutions to the problems are given as

$$\hat{\mathbf{m}}_0 = (\mathbf{L}_0'\mathbf{L}_0)^{-1}\mathbf{L}_0'\mathbf{d}_0 = (\mathbf{L}_0'\mathbf{L}_0)^{-1}\tilde{\mathbf{m}}_0 = \mathbf{H}_0^{-1}\tilde{\mathbf{m}}_0,$$

$$\hat{\mathbf{m}}_1 = (\mathbf{L}_1'\mathbf{L}_1)^{-1}\mathbf{L}_1'\mathbf{d}_1 = (\mathbf{L}_1'\mathbf{L}_1)^{-1}\tilde{\mathbf{m}}_1 = \mathbf{H}_1^{-1}\tilde{\mathbf{m}}_1, \tag{3}$$

where $\tilde{\mathbf{m}}_0$ and $\tilde{\mathbf{m}}_1$ are the migrated images, $\hat{\mathbf{m}}_0$ and $\hat{\mathbf{m}}_1$ are the least-squares inverse images, $\mathbf{L}_0'$ and $\mathbf{L}_1'$ are the migration operators, while $\mathbf{H}_0 = \mathbf{L}_0'\mathbf{L}_0$ and $\mathbf{H}_1 = \mathbf{L}_1'\mathbf{L}_1$ are the Hessian matrices.

In the first approach, the inverse time-lapse image ($\Delta\hat{\mathbf{m}}$) is given by

$$\Delta\hat{\mathbf{m}} = \hat{\mathbf{m}}_1 - \hat{\mathbf{m}}_0. \tag{4}$$

In the second approach, we express the modeling of operation for the two surveys as follows:

$$\mathbf{L}_0\mathbf{m}_0 = \mathbf{d}_0,$$

$$\mathbf{L}_1(\mathbf{m}_0 + \Delta\mathbf{m}) = \mathbf{d}_1. \tag{5}$$

where $\mathbf{m}_0 + \Delta\mathbf{m} = \mathbf{m}_1$. In matrix form, we can write

$$\begin{bmatrix} \mathbf{L}_0 & 0 \\ \mathbf{L}_1 & \mathbf{L}_1' \end{bmatrix} \begin{bmatrix} \mathbf{m}_0 \\ \Delta\mathbf{m} \end{bmatrix} = \begin{bmatrix} \mathbf{d}_0 \\ \mathbf{d}_1 \end{bmatrix}. \tag{6}$$

The least-squares solution to equation 6 is given as

$$\begin{bmatrix} \mathbf{L}_0'\mathbf{L}_0 + \mathbf{L}_1'\mathbf{L}_1 & \mathbf{L}_1'\mathbf{L}_1 \\ \mathbf{L}_1'\mathbf{L}_1 & \mathbf{L}_1'\mathbf{L}_1 \end{bmatrix} \begin{bmatrix} \hat{\mathbf{m}}_0 \\ \Delta\hat{\mathbf{m}} \end{bmatrix} = \begin{bmatrix} \mathbf{L}_0' & \mathbf{L}_1' \\ 0 & \mathbf{L}_1' \end{bmatrix} \begin{bmatrix} \mathbf{d}_0 \\ \mathbf{d}_1 \end{bmatrix} = \begin{bmatrix} \tilde{\mathbf{m}}_0 + \tilde{\mathbf{m}}_1 \\ \tilde{\mathbf{m}}_1 \end{bmatrix}, \tag{7}$$

$$\begin{bmatrix} \mathbf{H}_0 + \mathbf{H}_1 & \mathbf{H}_1 \\ \mathbf{H}_1 & \mathbf{H}_1 \end{bmatrix} \begin{bmatrix} \hat{\mathbf{m}}_0 \\ \Delta\hat{\mathbf{m}} \end{bmatrix} = \begin{bmatrix} \tilde{\mathbf{m}}_0 + \tilde{\mathbf{m}}_1 \\ \tilde{\mathbf{m}}_1 \end{bmatrix}. \tag{8}$$

This, may be re-arranged as follows:

$$\begin{bmatrix} \hat{\mathbf{m}}_0 \\ \Delta\hat{\mathbf{m}} \end{bmatrix} = \begin{bmatrix} \mathbf{H}_0 + \mathbf{H}_1 & \mathbf{H}_1 \\ \mathbf{H}_1 & \mathbf{H}_1 \end{bmatrix}^{-1} \begin{bmatrix} \tilde{\mathbf{m}}_0 + \tilde{\mathbf{m}}_1 \\ \tilde{\mathbf{m}}_1 \end{bmatrix}. \tag{9}$$

DISCUSSION

Although it is not feasible to explicitly compute the inverse matrix in equation 9, an iterative least squares solution of equation 8 is expected to yield reasonably good results for $\hat{\mathbf{m}}_0$ and $\Delta\hat{\mathbf{m}}$. In the 2D case considered, for a given frequency ω and an image-point $i(x,z)$, the measured data $\mathbf{d}(i_s, i_r)$ in equation is given by

$$\mathbf{d}(i_s, i_r; \omega) = \mathbf{L}\mathbf{m}_{i_{xz}} = \sum_{i_{xz}} \mathbf{G}(i_{xz}, i_\mathbf{s}; \omega)\mathbf{G}(i_{xz}, i_\mathbf{r}; \omega)\mathbf{m}_{i_{xz}}, \tag{10}$$

where $\mathbf{G}(i_{xz}, i_\mathbf{s}; \omega)$ and $\mathbf{G}(i_{xz}, i_\mathbf{r}; \omega)$ are the Green's functions from the shot and receiver positions ($i_s(x_s, 0)$ and $i_s(x_r, 0)$) respectively.

The Hessian sub-matrices ($\mathbf{H}_0$ and $\mathbf{H}_1$), which are the second derivatives of the cost functions (equations and 2) with respect to the model parameters $\mathbf{m}_{i_{xz}}$ and $\mathbf{m}_{j_{xz}}$ (where j_{xz} is some other point in the model space), may be computed as follows:

$$\mathbf{H}(i_{xz}, j_{xz}) = \sum_{\omega} \sum_{i_s} \mathbf{G}'(i_{xz}, i_s; \omega)\mathbf{G}(j_{xz}, i_s; \omega) \sum_{i_r} \mathbf{G}'(i_{xz}, i_r; \omega)\mathbf{G}(j_{xz}, i_r; \omega). \tag{11}$$

Using a target-oriented approach and limiting the computation to near-diagonal elements (Valenciano et al., 2006), equation 11 is reduced to

$$\mathbf{H}(i_T, i_T + a_i) = \sum_{\omega} \sum_{i_s} \mathbf{G}'(i_T, i_s; \omega)\mathbf{G}(i_T + a_i, i_s; \omega) \sum_{i_r} \mathbf{G}'(i_T, i_r; \omega)\mathbf{G}(i_T + a_i, i_r; \omega), \tag{12}$$

where a_i is the offset from the target image-point i_T.

Computation of the target-oriented wave-equation Hessian is discussed in detail by Valenciano and Biondi (2004). Hence, it is possible to compute the matrix of Hessian terms in equation 8 for specific targets of interest (e.g. regions around a sub-salt reservoir) and therefore compute the least-squares time-lapse image, $\Delta\hat{\mathbf{m}}$. Since the geometry (and other unwanted) information are contained in the Hessian terms, it should be possible to such effects from the time-lapse image by solving the inverse problem in equation 9 (or practically by solving equation 8 in a least-squares sense). The inversion technique is itself limited by the amount of good quality data from the sub-salt reflectors, but we expect that it provides better results than presently obtainable with migration. We intend to compare results from the inversion schemes with those from standard cross-equalization and to determine whether our techniques could make seismic monitoring of sub-salt reservoirs a reality.

CONCLUSIONS

Sub-salt reservoir monitoring of hydrocarbon reservoirs is a major challenge. We propose the computation of the time-lapse image either as a difference between inverse images or as a solution to a least-squares inverse problem. By solving for the time-lapse response through inversion (rather than a difference between two adjoint operations) it may be possible to obtain more reliable amplitude information and to correct for geometry and other effects which have heretofore limited seismic monitoring of sub-salt reservoirs. Suitable regularization and/or preconditioning may be used to better constrain the inversion result and to potentially reduce the required number of iterations in the inversion scheme. It may also be possible to structure the regularization operator to account for geomechamical and other changes outside the reservoir.

ACKNOWLEDGMENTS

Thanks to Alejandro Valenciano whose previous work and advice are helping get this research started and to Bob Clapp for many useful suggestions.

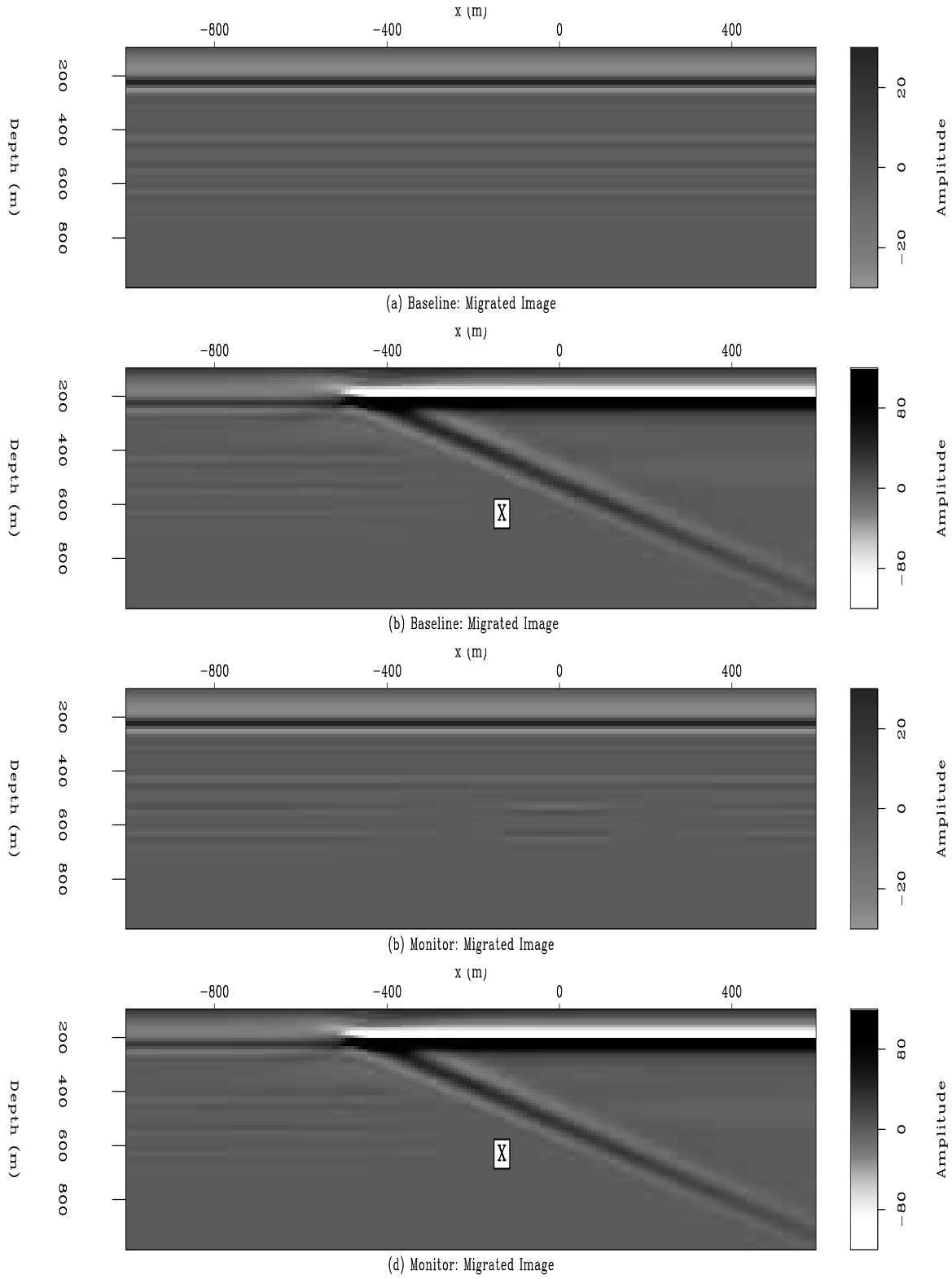

Figure 3: Migrated Images for velocity models in Figure 2. Survey direction: right to left. Data migrated using the correct (smoothed) velocity models. (a) and (b) Baseline; (c) and (d) Monitor. Notice the poor illumination of the reflectors close to the salt flank (region marked 'X' in (b) and (d). gayeni1-GboyeImg [ER]

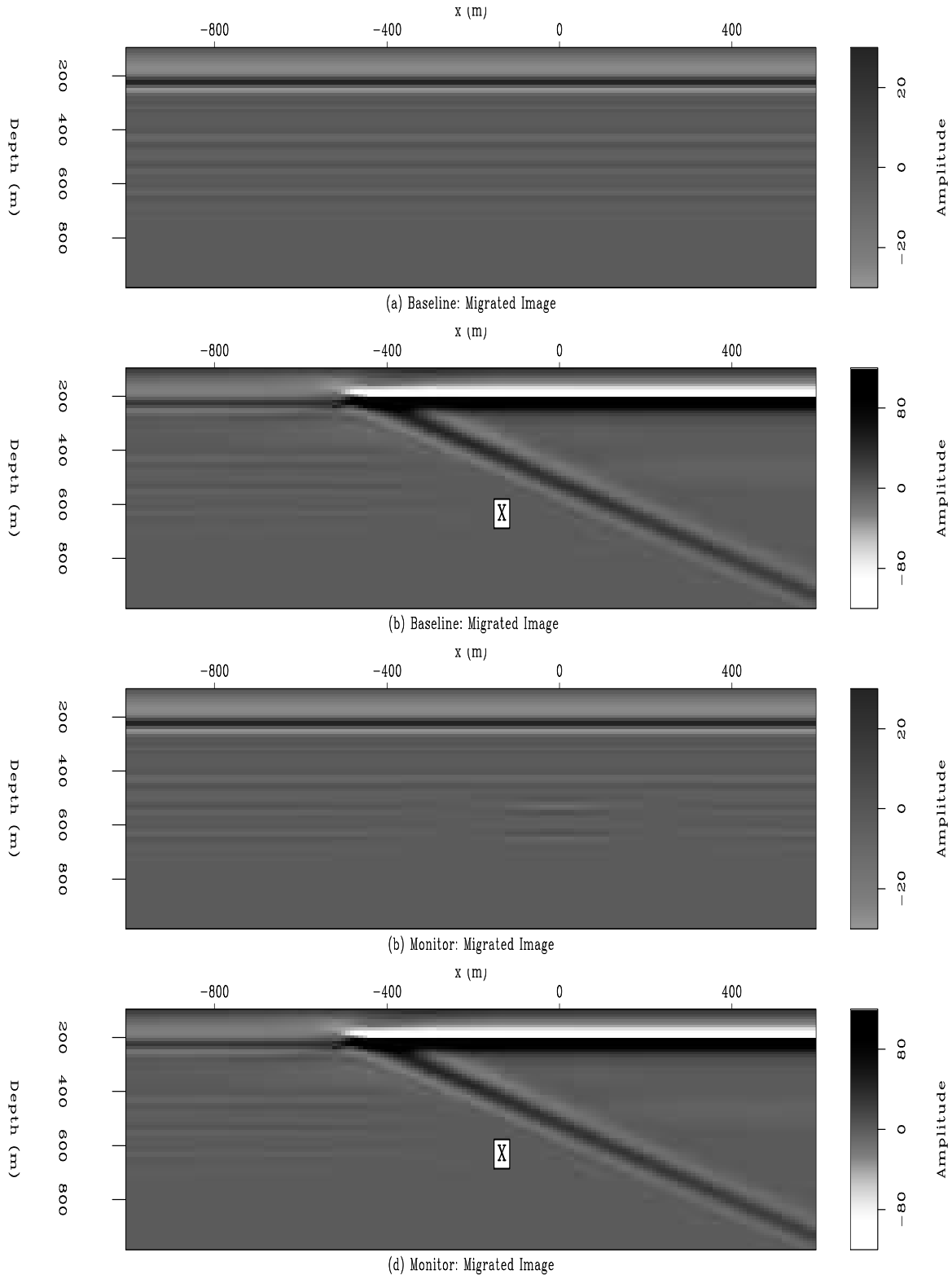

Figure 4: Migrated Images for velocity models in Figure 2. Survey direction: left to right. Data migrated using the correct (smoothed) velocity models. (a) and (b) Baseline; (c) and (d) Monitor. Note the poor illumination of the reflectors close to the salt flank (region marked 'X' in (b) and (d). gayeni1-GboyeImg2 [ER]

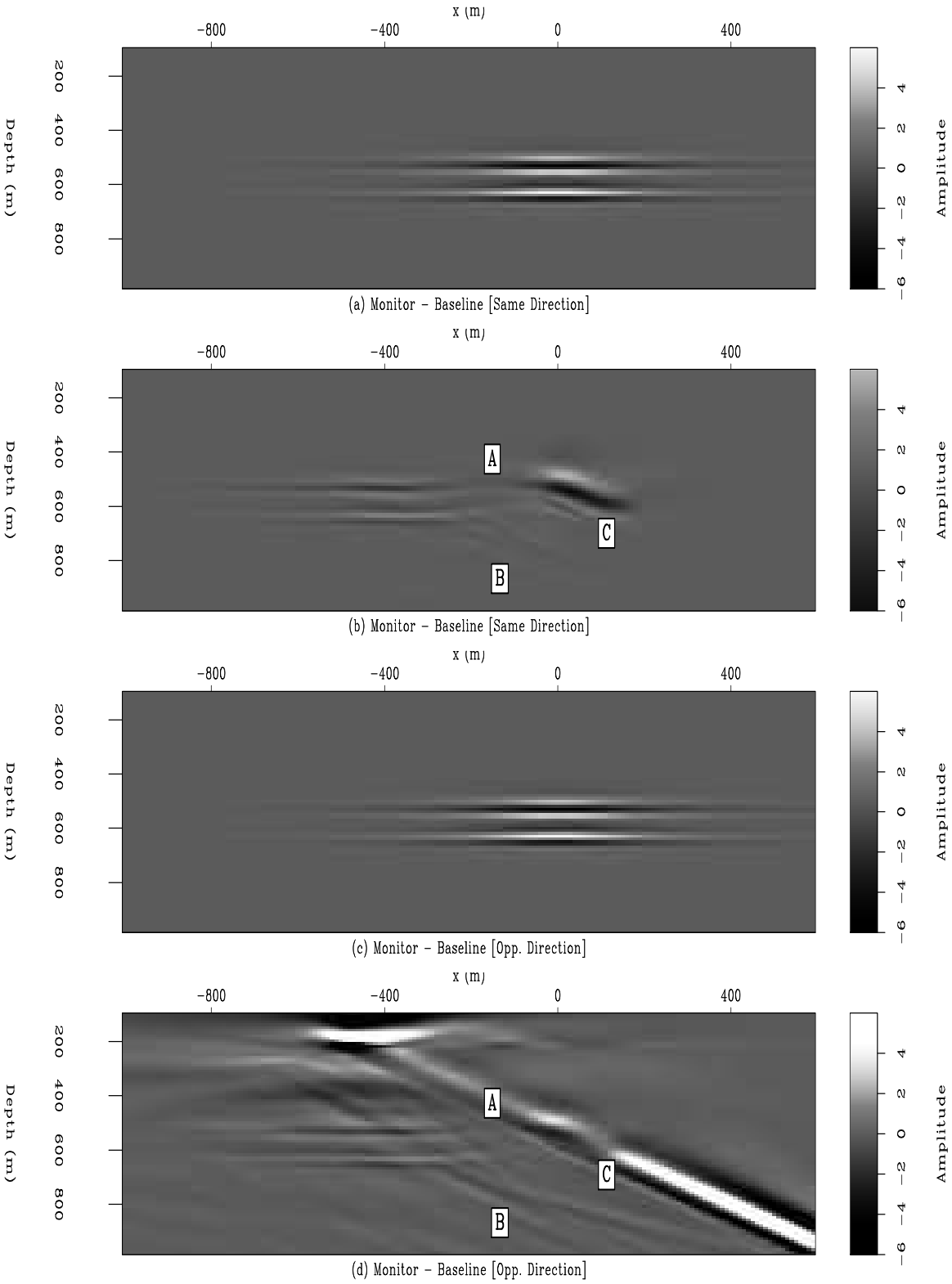

Figure 5: Raw difference Images (with and without the salt wedge) for same (a and b) and opposite (c and d) acquisition directions. Data migrated with the correct velocity models. Note the weak time-lapse response close to the reservoir (a result of the poor illumination) in the region marked 'A'. gayeni1-GboyeFB [ER]

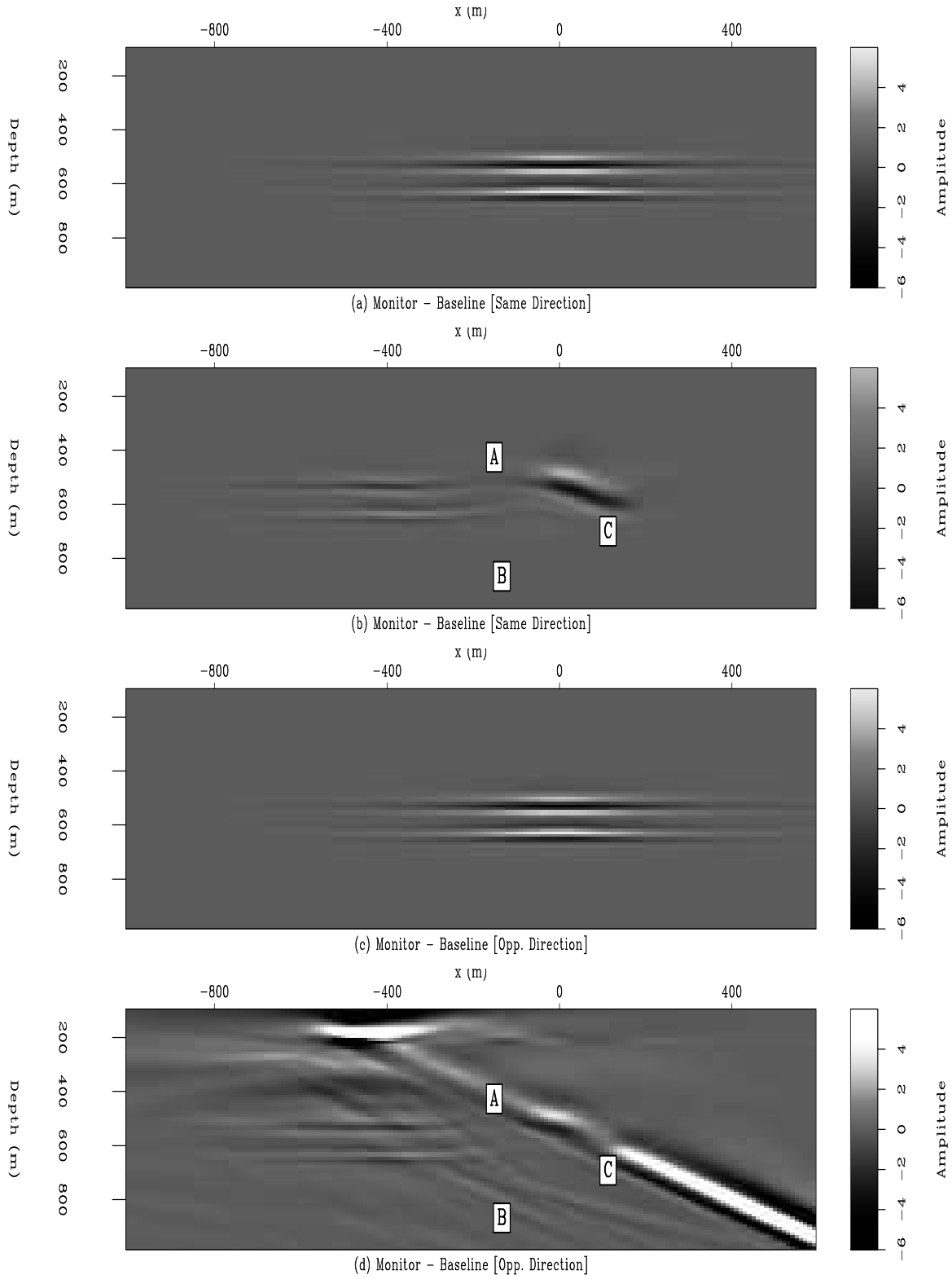

Figure 6: Raw difference Images (with and without the salt wedge) for same (a and b) and opposite (c and d) acquisition directions. Data migrated with the smoothed baseline velocity models. Note the differences in migration artifacts between Figures 5b and 6b in the regions marked 'B' and 'C'. gayeni1-GboyeSFB [ER]

REFERENCES

Batzle, M. and Z. Wang, 1992, Seismic properties of pore fluids: Geophysics, **57**, no. 11, 1396–1408.

Biondi, B., G. Mavko, et al., 1998, Reservoir monitoring: A multidisciplinary feasibility study: The Leading Edge, **17**, no. 10, 1404–1414.

Biondi, B., M. Prucha, and P. C. Sava, 1999, 3D wave-equation prestack imaging under salt.: 6th International Congress, Brazilian Geophysical Society.

Calvert, R., 2005, Insights and methods for 4D reservoir monitoring and characterization: SEG/EAGE DISC (Distinguished Instructor Lecture Course).

Claerbout, J. F., 2004, Image estimation by example: Geophysical soundings image construction: multidimensional autoregression:, http://sepwww.stanford.edu/sep/prof/gee/toc_html/.

Clapp, M. L., 2005, Imaging under salt: illumination compensation by regularized inversion: Ph.D. thesis, Stanford University, http://sepwww.stanford.edu/public/docs/sep122/paper_html/index.html.

Eastwood, J., P. Lebel, A. Dilay, and S. Blakeslee, 1994, Seismic monitoring of steam-based recovery of bitumen: The Leading Edge, **13**, no. 04, 242–251.

Eiken, O., G. U. Haugen, M. Schonewille, and A. Duijndam, 2003, A proven method for acquiring highly repeatable towed streamer seismic data: Geophysics, **68**, no. 4, 1303–1309.

Johnston, D., 2005, Time-lapse 4D technology: Reservoir surveillance: AAPG Search and Discovery.

Laws, R. and E. Kragh, 2000, Rough seas and time-lapse seismic: Rough seas and time-lapse seismic:, Eur. Assn. Geosci. Eng., 62nd Mtg., Session:L0015.

Lefeuvre, F., Y. Kerdraon, et al., 2003, Improved reservoir understanding through rapid and effective 4D: Girassol field, Angola, West Africa: SEG Technical Program Expanded Abstracts, **22**, no. 1, 1334–1337.

Lumley, D. E., 1995, Imaging under salt: illumination compensation by regularized inversion: Ph.D. thesis, Stanford University, http://sepwww.stanford.edu/public/docs/sep91/.

Malaguti, R., M. Allen, A. Litvin, and C. Gregory, 2001, Sub-salt imaging using 3D pre-stack depth migration in the Uk Southern North Sea - a case history: First Break, **19**, no. 05, 253–258.

Muerdter, D. and D. Ratcliff, 2001, Understanding subsalt illumination through ray-trace modeling, Part 3: Salt ridges and furrows, and the impact of acquisition orientation: The Leading Edge, **20**, no. 8, 803–816.

Ratcliff, D. W., C. A. Jacewitz, and S. H. Gray, 1994, Subsalt imaging via target-oriented 3-D prestack depth migration: The Leading Edge, **13**, no. 03, 163–170.

Rickett, J. and D. E. Lumley, 2001, Cross-equalization data processing for time-lapse seismic reservoir monitoring: A case study from the Gulf of Mexico: Geophysics, **66**, no. 4, 1015–1025.

Rickett, J., 2003, Illumination-based normalization for wave-equation depth migration: Geophysics, **68**, 1371–1379.

Ross, C. P. and M. S. Altan, 1997, Time-lapse seismic monitoring: Some shortcomings in nonuniform processing: The Leading Edge, **16**, no. 06, 931–937.

Sava, P., 2006, Subsalt exploration and development: Imaging, interpretation, and drilling—What have we learned? 2006 SEG/EAGE summer research workshop: The Leading Edge, **25**, no. 11, 1370–1376.

Tarantola, A., 1987, Inverse problem theory: Methods for data fitting and model parameter estimation: Elsevier Science Publication Company, Inc.

Valenciano, A. A. and B. Biondi, 2004, Target-oriented computation of the wave-equation imaging Hessian: SEP–**117**, 63–76.

Valenciano, A. A., B. Biondi, and A. Guitton, 2006, Target-oriented wave-equation inversion: Geophysics, **71**, A35–A38.

Whitcombe, D. N., J. M. Marsh, et al., 2004, The systematic application of 4D in BP's North-West Europe operations — 5 years on: SEG Technical Program Expanded Abstracts, **23**, no. 1, 2251–2254.

Zou, Y., L. R. Bentley, L. R. Lines, and D. Coombe, 2006, Integration of seismic methods with reservoir simulation, Pikes Peak heavy-oil field, Saskatchewan: The Leading Edge, **25**, no. 6, 764–781.